ORCA – Online Research @ Cardiff

The Agadir Slide offshore NW Africa: Morphology, emplacement dynamics and its potential contribution to the Moroccan Turbidite System

Wei Li[a,b,*], Sebastian Krastel[b], Tiago M. Alves[c], Morelia Urlaub[d], Lisa Mehringer[e], Anke Schürer[e], Peter Feldens[f], Felix Gross[b], Christopher J. Stevenson[g], Russell B. Wynn[h]

[a] Key Laboratory of Ocean and Marginal Sea Geology, South China Sea Institute of Oceanology, Chinese Academy of Sciences, 510301 Guangzhou, P.R. China
[b] Christian-Albrechts-Universität zu Kiel, Institute of Geosciences, Otto-Hahn-Platz 1, 24118 Kiel, Germany
[c] 3D Seismic Lab. School of Earth and Ocean Sciences, Cardiff University, Main Building, Park Place, Cardiff, CF10 3AT, United Kingdom
[d] GEOMAR Helmholtz Centre for Ocean Research Kiel, Wischhofstr. 1-3, 24148 Kiel, Germany
[e] Faculty of Geosciences and MARUM, Center for Marine Environmental Sciences, University of Bremen, Klagenfurter Straße, 28359 Bremen, Germany
[f] Leibniz Institute for Baltic Sea Research, Warnemünde, 18119 Rostock, Germany
[g] School of Earth, Ocean and Ecological Sciences, University of Liverpool, Liverpool L69 3GP, United Kingdom
[h] National Oceanography Centre, European Way, Southampton, Hampshire SO14 3ZH, United Kingdom
*Correspondence to: Dr. Wei Li (wli@scsio.ac.cn)

Abstract

A newly identified large-scale submarine landslide on the NW African margin (Agadir Slide) is investigated in terms of its morphology, internal architecture, timing and emplacement processes by using high-resolution multibeam bathymetry data, 2D seismic profiles and gravity cores. The Agadir Slide is located south of the Agadir Canyon at a water depth ranging from 500 m to 3500 m, with an estimated affected area of ~5500 km^2. The complex morphology of the Agadir Slide reveals two headwall areas and two slide fairways (Western and Central slide fairways). Volume calculations indicate that approximately 340 km^3 of sediment were accumulated downslope in the slide fairways (~270 km^3) and Agadir Canyon (~70 km^3). Novel stratigraphic correlations based on five gravity cores indicate an age of ~142±1 ka for the emplacement of the Agadir Slide. However, the emplacement dynamics of the Agadir Slide suggests it was developed in two distinct, successive stages. The presence of two weak layers (glide planes) is suggested as the major preconditioning factor for the occurrence of slope instability in the study area, and local seismicity related to fault activity and halokinesis likely triggered the Agadir Slide. Importantly, the Agadir Slide neither disintegrated into sediment blocks nor was transformed into turbidity currents. Its timing of emplacement does not correlate with any turbidites recorded downslope across the Moroccan Turbidite System.

Keywords: Agadir submarine slide; Turbidity current; Agadir slide; Moroccan Turbidite System; Northwest Africa.

1 Introduction

Submarine landslides are ubiquitous across continental margins (Hampton et al., 1996; Masson et al., 2006; Krastel et al., 2014). They comprise one of the key mechanisms transporting sediment from continental shelves and upper slope areas into deep-sea basins (Masson et al., 2006). Submarine landslides can generate damaging tsunamis affecting local and distal coastal communities and associated infrastructure (Mosher et al., 2010; Tappin et al., 2014). At local scales, large-volume and fast-moving submarine landslides can disintegrate to produce turbidity currents through mixing processes with the surrounding sea water (Talling et al., 2007a; Clare et al., 2014). Turbidity currents are more mobile than their parent landslides and capable of transporting sediment over thousands of kilometers to reach distal Abyssal Plains (Talling et al., 2007b; Wynn et al., 2010; Stevenson et al., 2014).

The Moroccan Turbidite System extends 1500 km from the head of the Agadir Canyon to the Madeira Abyssal Plain (Fig. 1), and it has hosted some of the largest (with volumes exceeding 150 km^3) landslide-triggered turbidity currents occurring in the past 200 ka (Wynn et al., 2002; Talling et al., 2007a; Frenz et al., 2009; Wynn et al., 2010;

Stevenson et al., 2014). The Moroccan Turbidite System fills three interconnected sub-basins: the Seine Abyssal Plain, the Agadir Basin and the Madeira Abyssal Plain (Wynn et al., 2002; Fig. 1). A robust geochemical and chronostratigraphic framework has been developed across the Moroccan Turbidite System, allowing individual turbidite beds to be correlated across the continental margin (Wynn et al., 2002; Frenz et al., 2009; Hunt et al., 2013a). The turbidites are sourced from three areas (Fig. 1): (1) organic-rich siliciclastic flows sourced from the Moroccan margin, fed into the system via the Agadir Canyon and several submarine canyons (Wynn et al. 2002; Frenz et al., 2009; Hunt et al., 2013a); (2) volcaniclastic flows sourced from either the Canary Islands or Madeira (Hunt et al., 2013b), and (3) carbonate-rich flows sourced from local seamounts (Wynn et al., 2002). The first group represents the largest deposits, and due to their large volumes, their sources are most likely submarine landslides originating from the upper parts of the Moroccan continental slope (Talling et al. 2007a). However, to date no major landslide scars have been documented in the upper parts of the system.

The study area is situated on the Moroccan continental margin at water depths ranging from 30 m to more than 4000 m (Fig. 1). A large-scale submarine landslide (Agadir Slide) was recently identified in this area based on hydroacoustic data (Fig. 2; Krastel et al., 2016). However, many questions are still to address, such as (i) how the Agadir Slide was emplaced and (ii) whether the Agadir Slide was a source landslide for turbidites in the Moroccan Turbidite System. In this contribution we combine high-resolution multi-beam bathymetry, 2D seismic profiles, and gravity cores with the aim to: a) investigate the detailed seafloor morphology of the Agadir Slide, b) describe the internal architecture of the Agadir Slide and estimate its volume, c) determine the timing of the Agadir Slide, and d) discuss the emplacement processes and flow behaviour of the Agadir Slide.

2. Geological setting

2.1 The Northwest African margin

The Northwest (NW) African margin is characterised by a flat continental shelf, generally 40-60 km wide, and a shelf break at a water depth of 100 to 200 m (Seibold, 1982; Hühnerbach and Masson, 2004). The continental slope has a width of 50-250 km beyond the shelf break, and records a slope gradient of 1-6° (Fig. 1; Dunlap et al., 2010). The continental slope continues into the continental rise at water depths of 1500 to 4000 m, with gradients ranging from about 1° on the lower slope/upper rise to 0.1° on the lower rise (Seibold, 1982). The continental rise is generally 100-1500 km wide, and terminates at a water depth of 4500-5400 km, beyond which occurs the flat expanse of the Agadir Basin, the Seine Abyssal and Madeira Abyssal Plains (Fig. 1).

The NW African margin is dissected by numerous canyons and channels, and interrupted by multiple volcanic islands and seamounts, creating a topographically complex setting that greatly influences local sedimentary processes (Wynn et al., 2000). Prominent bathymetric features near the study area include a group of volcanic seamounts to the west and the Canary Islands to the southwest (Fig. 1). The Agadir Canyon extends from the edge of the shelf break down to the upper continental rise, opening out into the Agadir Basin (Wynn et al., 2000; Krastel et al., 2016) (Fig. 1). The Agadir Basin occupies water depths of about 4400 m, has an area of 22, 000 km² and is almost flat, having a gradient of just 0.02°. The Seine Abyssal Plain is also located at a water depth of around 4400 m with an area of 68, 000 km². The Madeira Abyssal Plain is the largest deep sea basin in the region, occupying water depths of around 5400 m and covering an area of 68, 000 km² (Rothwell et al., 1992). It is extremely flat, with a slope of less than 0.01°, and a surface relief varying by less than 10 m. The Agadir Basin and Madeira Abyssal Plain are connected by a 600-km long network of shallow channels termed the Madeira Distributary Channel System (Masson, 1994;

Wynn et al., 2000; Stevenson et al., 2013).

The Moroccan margin has experienced multiple deformational episodes associated with toe-thrust anticlines during the Cretaceous and the Cenozoic (Tari and Jabour, 2013). The renewed uplift and neotectonics inversion of the Atlas Mountains that tilts the margin towards the deep water and causes the ongoing deformation of salt structures (Tari and Jabour, 2013). As a result of tectonic movements, the NW African continental margin has been a region of slope instability during the Quaternary and some of the World's largest submarine landslides have occurred in the region over the past 200 ka (Krastel et al., 2012). Some of NW Africa's submarine landslides transformed into highly mobile turbidity currents soon after slope failure (Wynn et al., 2002), whereas others remained as coherent slide blocks (Alves, 2015). Yet, not all the landslides have essentially the same composition. For example, the Sahara Slide offshore Western Sahara has a run-out distance of up to 900 km, it failed as a translational slide and disintegrated into a plastic debris flow. However, there is no evidence for its transformation into a turbidity current (Gee et al., 1999; Georgiopoulou et al., 2010). The way in which submarine landslides are emplaced has important implications for tsunami genesis. For geohazard assessments it is also important to understand why some landslides form turbidity currents and others do not, as turbidity currents can travel at relatively high speeds (tens of m/s) and pose a major geohazard to sea floor infrastructure such as telecommunication cables and pipelines (Piper et al., 1999).

2.2 The Moroccan Turbidite System

The Moroccan Turbidite System on the northwest African continental margin is one of the longest turbidite systems in the world and it has a total length of 1500 km (Fig. 1; Wynn et al., 2002). The morphology of Moroccan Turbidite System is largely controlled by the position of volcanic islands, seamounts and salt diapirs (Wynn et al.,

2000). The Moroccan Turbidite System extends along three interlinked deep-water basins: the Agadir Basin, the Seine Abyssal Plain and the Madeira Abyssal Plain (Wynn et al., 2002).

The Moroccan Turbidite System shows a relatively low turbidite frequency of ~ 1 event every 15,000 years (Wynn et al., 2002), and the turbidites are separated by discrete hemipelagic intervals (Frenz et al., 2009; Hunt et al., 2013a). Fourteen turbidite beds (AB1 to AB14) have been identified in the Moroccan Turbidite System during the past 200 ka (Wynn et al. 2002; Talling et al. 2007a; Hunt et al. 2013a). Most of these turbidites were sourced from the Moroccan margin, including AB3 and AB4 during the Marine Isotope Stage (MIS) 3, AB5 at ~60 ka, AB 6 during the MIS 4/5, and AB7, AB 9, AB11 to AB13 during the MIS 5 (Wynn et al., 2002; Frenz et al., 2009).

Turbidite AB12 is the largest turbidite in the Moroccan Turbidite System and contains ~230 km^3 of sediment (Frenz et al., 2009). AB1 (~1 ka; Thomson and Weaver, 1994) was suggested to be sourced from the continental margin south of the Canary Islands and related to the recent re-activation of Sahara Slide (Frenz et al., 2009). Turbidite AB2 (~15 ka) is volcanoclastic and is likely sourced from the El Golfo landslide around the western Canary Islands (Frenz et al., 2009). The AB8 (during the MIS 5) originated from relatively localised failure of a presorted volcaniclastic sand sourced from the flanks of Madeira (Frenz et al., 2009; Hunt et al., 2013a). AB10 (during the MIS 5) occurred throughout the Agadir Basin except along the northern margin and the Agadir Canyon mouth (Frenz et al., 2009). Turbidite AB 14 is interpreted as being deposited at ~160 ka and is likely to be sourced from the Icod landslide on the northeast flank of Tenerife.

3. Data and methods

The data set used in this study was collected offshore northwest Morocco during the Maria S. Merian research cruise MSM32, in October 2013. The dataset comprises multibeam bathymetry data, 2D seismic profiles and gravity cores (Figs. 2 and 3).

3.1 Multibeam bathymetry data

During cruise MSM32, a hull-mounted Kongsberg Simrad system EM122 was used for accurate bathymetric mapping. The EM122 system works with a nominal frequency of 12 kHz and an angular coverage sector of up to 150° and 864 soundings per ping. The multibeam bathymetry data cover about 13,000 km², from the Agadir Slide headwall area at a water depth of 600 m, down to the Agadir Canyon at a water depth of 4500 m (Fig. X). The multibeam data was processed by using the QPS FLEDERMAUS and MBSYSTEM software. Included in the processing were general quality checks (navigation, attitude data and sound velocity profiles), the generation of a CUBE surface, and the removal of spikes, especially at the overlapping parts of individual profiles. The acquired bathymetric data were gridded for visualisation and subsequent volume calculations. A 30 m by 30 m grid of bathymetric data was generated and geographically placed in relation to the WGS84 ellipsoid.

The pre-slide topography was generated at a later stage by using the minimum-curvature splines in tension interpolation (Smith and Wessel, 1990). The estimated volumes of evacuated sediment in the Agadir headwall area and the Central slide fairway were obtained by subtracting the interpolated surface from the seafloor topography (Fig. 2).

3.2 2D seismic data

An 88-channel, 137.5 m-long Geometrics GeoEel streamer, and a standard GI-gun (primary volume of 1.7 L), were used to acquire high-resolution multichannel seismic data. In total, fifty-six two-dimensional (2D), high-resolution multi-channel seismic profiles, with an entire length of about 1500 km, were acquired during this cruise. Signal processing used the VISTA® 2D/3D Seismic Data Processing Software. Basic processing steps included trace binning at 12.5 m, filtering, gain recovery with increasing depth, NMO-correction, stacking and post-stack finite-difference (FD) migration. IHS Kingdom® software was used to visualise and interpret the seismic data. The top and bottom surfaces of the Agadir Slide were interpreted along all seismic lines and gridded by using the minimum curvature gridding algorithm (Smith and Wessel, 1990). The volumes of the Agadir Slide deposits accumulated in the Central slide fairway, Western slide fairway and Agadir Canyon were estimated by subtracting the grids created from the top and bottom surfaces of the Agadir Slide. The seismic velocity used for time-depth conversion was 1650 m/s.

3.3 Gravity cores

Three gravity cores (MSM32-8-2, MSM32-28-1 and MSM32-14-1) up to 10 m long were recovered in the Agadir Slide area (Fig. 3). Another two gravity cores (GeoB 2415-2 and GeoB4216-1) located in the immediate vicinity of the Agadir Slide were also examined (Fig. 3). They were obtained during the RV METEOR cruise 37/38 in 1997 (Wefer et al., 1997). Magnetic Susceptibility was measured in 2 cm-intervals using a handheld Magnetic Susceptibility Meter SM 30 from ZH Instruments. Magnetic Susceptibility measurements on cores GeoB 4215-2 and GeoB 4216-1 were obtained from Kuhlmann et al. (2004) and Freudenthal et al. (2002), respectively. All studied cores were correlated across the study area to understand the stratigraphic framework of the Agadir Slide. Correlation framework was developed using down core magnetic susceptibility profiles, distinct colour changes in sediment, sedimentary properties and key sedimentary structures. GeoB cores had established age models (Freudenthal et al., 2002; Kuhlmann et al., 2004) that were extrapolated to the MSM32 cores, which provided an age model for the emplacement of the Agadir Slide.

4. Morphology of the Agadir Slide

The Agadir Slide extends from 500 m to 3500 m water depth, along 350 km covering an area of ~5000 km² (Fig. 2). The Agadir Slide is located ~200 km south of the Agadir

Canyon. It is bounded to the south by a prominent sidewall cut into the continental slope (Figs. 2 and 3a). The Agadir Slide can be divided into four domains: (i) upper headwall area, (ii) lower headwall area, (iii) Western slide fairway, and (iv) Central slide fairway (Fig. 3a and b). In addition, five seamounts, named as SM 1 to 5, can be identified on the seafloor, affecting the morphology of the Agadir Slide (Fig. 3a). The terminology of fairway used in this study is considered as the pathway of debris flows, which can be clearly imaged on the bathymetrical map (Krastel et al., 2016).

The upper headwall area is located at a water depth of 500 m to 1600 m (Fig. 3a). The width of the headwall area is ~2 km in the upper part and increases gradually to approximately 35 km downslope, giving the headwall area an overall V-shape in plan view (Fig. 3a). It has a length of 40 km and covers an area of approximately 560 km^2. The height of the headwall scarp in the domain (i) is ~125 m (Fig. 4a). The slope gradient within the headwall area varies between 0.6° and 4° (Fig. 3b). Seafloor morphology within the headwall area is smooth and few slide blocks can be recognised. In contrast, several submarine canyons and a field of sediment waves developed upslope of the upper headwall area of Agadir Slide (Fig. 4a). The sidewall scarp in the eastern border of the upper headwall area is ~35 km in length and shows an N-S orientation. The western sidewall scarp has a length of ~40 km and its orientation changes from NNW to NW at a water depth of 1250 m. Both sidewall scarps have a height of up to 90 m and they disappear gradually downslope (Figs. 3a and 4a). Several (minor) slide scars are identified close to the upper headwall area, and in the northwestern corner of the Central slide fairway (Figs. 3a and b).

The lower headwall area is located at a water depth of 1800 m to 1950 m and it has a width of ~9 km (Fig. 4b). The sidewall scarps of the lower headwall area are bordered by SM 3 to the west and by SM 4 to the southwest. The headwall scarp in the lower headwall area has a height of ~100 m (Fig. 4b).

The Western slide fairway can be considered as the northwest continuation of the Agadir Slide headwall at a water depth of ~1750 m (Figs. 3a and b). It is bounded by SM 1 and SM 2 to the south, and by the western sidewall scarp of the Central slide fairway to the east. Its western border is characterised by the formation of positive relief when compared to the adjacent seafloor (Fig. 2a). It covers an area of 1250 km^2 and it has a length of ~65 km. The width of the Western slide fairway increases downslope to a maximum value of 30 km at ~1950 water depth and then decreases gradually (Fig. 3a). It then decreases gradually downslope (Fig. 3a). The regional slope gradient within the Western slide fairway also decreases from 0.6° to 0.2° downslope (Fig. 3b). The seafloor surface is smooth with only one pronounced incision surface, with a depth of ~20 m, identified close to the headwall area (Fig. 3a). The western boundary of the Western slide fairway shows a positive relief of ~9 m compared to the nearby undeformed seafloor (Fig. 4c).

The Central slide fairway connects the Agadir Slide headwall area to the Agadir Canyon; it is the major pathway for slide deposits travelling into the Agadir Canyon (Fig. 3a and b). Distinctive sidewall scarps can be identified in the northern and southern parts of the Central slide fairway, with heights ranging from 30 m to 50 m. In the middle part, its orientation changes from N-S to NE-SW and seafloor morphology changes from distinctive sidewall scarps into a series of features with positive relief (~15 m) at water depths of 2100-2200 m (Figs. 3a and 4d). Further to the north, the Central slide fairway entered the Agadir Canyon with a noticeable change in slope gradient from 0.5° to 1.8°, at a water depth of ~2500 m (Figs. 3b and 7b). A pronounced NW-trending slide scarp is also identified in the eastern part of the Central slide fairway (Fig. 3a).

5. Internal architecture of the Agadir Slide

The internal seismic character of the Agadir Slide deposits is characterised by a highly disrupted to chaotic and transparent

seismic facies, and is bounded above, below and laterally by continuous strata (Figs. 5, 6 and 7). The sediments draped above the mass-transport deposits generated by Agadir Slide show almost consistent thickness from all the seismic profiles (Figs. 5, 6 and 7). Two basal shear surfaces (named as BSS I and BSS II) are recognized, and each forms a continuous plane that dips parallel to the underlying strata (Figs. 5b, 6a, b and c). These two basal shear surfaces are located at different stratigraphic depth and BSS II is deeper than BSS I (Figs. 6a and b). Erosional remnants are identified on the downslope side of SM 3 and the western boundary of Central slide fairway and they seem to separate BSSI and BSSII (Figs. 6a and b). The BSS I extends from the upper headwall area to the Western slide fairway (Figs. 3b and 4c), while BSS II can only be identified in the Central slide fairway (Figs. 3b, 5b and c).

The thickness of the Agadir Slide deposits in the upper headwall area is quite thin compared to those in the Western and Central slide fairway. Numerous faults can be recognised on the crests of the salt domes (Figs. 6b and c). Several faults propagated vertically and terminated on the basal shear surfaces of the Agadir Slide. The Agadir Slide deposits are affected by several salt diapirs (Figs. 5b, c and 6b). At some places, the slide deposits seem to be elevated by the salt diapir, which may indicate the activation of the salt diapirs during or after the occurrence of the Agadir Slide (Fig. 5b). Multiple small-scale faults can be identified in the toe region of the Central slide fairway (Fig. 6c). Based on the seismic line direction, the orientations of these faults could be roughly parallel to the sliding direction in plan view. On the eastern flank of the Central slide fairway, slide material accumulated higher than the surrounding unaffected sea floor, forming a marked positive relief above the original sea bed (Figs. 6c, d and 7a).

6. Volume estimations

Evacuated material: The pre-slide bathymetry within the Agadir Slide headwall area, and the Central slide fairway, are here reconstructed to estimate the total evacuated volume (Figs. 8a and b). A total volume of ~36 km^3 of sediment was evacuated from the Agadir Slide headwall area affecting an area of ~560 km^2 (Fig. 8a). This volume and area indicate an average thickness of 65 m for the removed sediment. Strata evacuated from the Central slide fairway have a volume of 135 km^3 and a mean height of 50 m (Fig. 8b). At the western and eastern border of the Central slide fairway, 0.4 km^3 of slide deposits with a mean height of 5 m are accumulated above the pre-slide topography.

Deposited material: The volume of the Agadir Slide deposits in the Central slide fairway, Western slide fairway and Agadir Canyon can be estimated based on the interpreted seismic data (Figs. 8c, d and e). In the headwall area, the thickness of the slide deposits is quite small (<25 m), indicating that erosion predominates deposition (Fig. 5a). The Agadir Slide deposits have a volume of 63 km^3 in the Western slide fairway and affect an area of ~1240 km^2 (Fig. 8c). The average thickness of the slide deposits in this area is ~51 m. In the Western slide fairway, the majority of the mobilized sediment was deposited close to its western flank and in its southern part, where the thickness of the slide deposits reaches up to 110 m (Fig. 8c). In the Central slide fairway, 206 km^3 of Agadir Slide deposits were accumulated over an area of 2970 km^2 with a mean thickness of 70 m (Fig. 8d). Most of the Agadir Slide deposits were distributed on in the eastern of the Central slide fairway (Fig. 8d). The volume and affected area of the slide deposits within the Agadir Canyon are 68 km^3 and 1686 km^2, respectively. The thickness of Agadir Slide deposits in the canyon varies greatly and it has an average thickness of 40 m. At the southern end, its thickness is less than 30 m and increases to about 40 m further north. The largest accumulation of slide deposits occurs at the northern border of the central part of the Agadir Canyon.

In summary, a total volume of 170 km^3 of sediments was evacuated, while 340 km^3 of sediments were deposited by the Agadir Slide.

7. Age model for the Agadir Slide

Sediment sampled in the gravity cores was divided in two units; Units A and B, based on visual core descriptions (Figs. 9a and b). Unit A, forming the upper part of the sediment cores, contains muddy carbonate-rich nannofossil ooze in various nuances of light brownish, reddish and greenish colors (Fig. 9a). Unit A is considered as a continuous succession of hemipelagic sediment comprising fine-grained biogenic and terrigenous material. Unit B is located in the lower part of the collected sediment cores and underlies Unit A (Fig. 9a). Sediment in Unit B is light beige, brownish, reddish, as well as greenish, foraminifera bearing, carbonate-rich nannofossil ooze (Fig. 9a). Unit B is deformed by slump folds and internal shearing. Unit B is thus interpreted as the Agadir Slide deposits.

Core GeoB4216 is located to the west of the study area in an area not affected by the Agadir Slide (Figs. 3a and 9b). The grain size ranges from silty mud to muddy fine-sand and layers are identified by varying sediment colours. Based on these observations, the whole core can be described as Unit A.

Magnetic Susceptibility was measured in Unit A to correlate the sediment-core data across the study area and to establish a stratigraphy (Fig. 9b). Magnetic Susceptibility data was not measured in Unit B as it consists of remobilized strata. Magnetic Susceptibility profiles in all studied cores show distinct tie-points, which can be correlated across the study area despite the fact that only relative values were measured for the MSM32 cores (Fig. 9b). The magnetic susceptibility correlation allowed the age model from the GeoB cores (Kuhlmann et al., 2004; Freudenthal et al., 2002) to be extrapolated to the MSM32 cores. The MSM32 cores show relatively constant sedimentation rates of 4.4, 4.0 and 4.1 cm/ka for cores MSM32-8, 28, and 14 respectively. The oldest Magnetic Susceptibility tie-point occurs between 5-12 cm above the Agadir Slide deposits and is dated at 140 ka. Assuming a similar sedimentation rate below this 140 ka horizon, an age of 142±1 ka is estimated for the emplacement of the Agadir Slide.

8. Flow history of the Agadir Slide

Our observations reveal that the Agadir Slide affects an area of ~5500 km^2, displaces a volume of 340 km^3 and shows a (run-out) distance of 350 km. The Agadir Slide can be considered as a large-scale submarine landslide as its size and volume are larger than almost 80-90% of the documented submarine landslides (Moscardelli and Wood, 2015). Different sources of sediments, i.e. localized and extrabasinal sources, have been proposed to contribute to the volume of the submarine landslides (Moscardelli and Wood, 2008).

The main contribution to the volume of Agadir Slide results from the mobilisation of sediments along the two basal shear surfaces (glide planes) in the headwall areas, Central and Western slide fairways. The extrabasinal source of sediments may relate to a variable sediment input from multiple minor slide events generated near the Agadir Slide's source area (Fig. 3a). These slide events may have generated additional sediments, later transported into the Western slide fairway, Central slide fairway and Agadir Canyon (Fig. 3a). In addition, salt diapirs are widespread in the Agadir Slide area and they have played a vital role on the morphology and evolution of the Agadir Slide. Strong erosional processes occurred along the flanks of the salt diapirs, which may enable the adding of material to the slide from the collapsing flanks of the salt diapirs. The erosional remnants that separate BSSI and BSSII could have been formed by the presence of salt diapirs that could have diverted the Agadir Slide (Fig. 6a). These erosional remnants are similar to the "erosional shadow remnants" at the base of the shallowest mass-transport complex in offshore Trinidad (Moscardelli et al., 2006). The presence of erosional remnants indicates the large-scale lateral erosive energy of Agadir Slide when passing the salt diapirs on the seafloor. These salt diapirs acted as physiographic barriers that prevented parts of the older sea floor from being eroded by passing mass-transport flows (Moscardelli et al., 2006).

The high-resolution imaging of the internal architecture of Agadir Slide allowed the investigation of its flow behaviour during the emplacement processes. A close interaction between submarine landslides and the sea floor can lead to the extensive remobilisation of pre-existing deposits on the sea bed (Watt et al., 2012; Alves et al., 2014). Widespread erosion of subsurface sediments by debris flows, leading to an increase in the flow volume, is capable of creating a basal layer upon which the overlying gravity flows can be moved over long distances (Masson et al., 2006). However, based on our observations, the BBS I and BBS II are roughly parallel to the stratification and they seem to correlate with the same stratigraphic level (Figs. 5 and 6). The zoomed section of seismic records does not show the basal shear surfaces take a big bite out of the underlying sediments. Thus, we propose that the flows associated with the slide deposition are supposed to be plastic, and they are not supposed to erode the substratum. The first slide event occurred in the upper headwall area did not transform into a debris flow and it just occurred as a slide along the BSS I. The second slide event also took place as a slide and moved downslope along the BSS II. It did not evolve into a debris flow at least before entering the Agadir Canyon.

Submarine landslides commonly disintegrate into slide blocks of variable sizes in their toe regions (Alves, 2015). However, few slide blocks can be recognized on the bathymetric data imaging the Agadir Slide (Fig. 3a). In reality, not all submarine landslides are transformed into long run-out turbidity currents either. The Sahara Slide occurred as a relatively slow-moving slab-type failure on a low-angle slope and the high cohesiveness of the fine-grained headwall sediments likely prevented it to disintegrate into turbidity currents (Georgiopoulou et al., 2010). The emplacement of the Agadir Slide may be similar to the Sahara Slide. No sufficient kinetic energy was available for transition into a turbidity current, and the erosion at the sidewalls of the slide may have dragged a lot of energy out of the system causing the slide to slow down. The orientation of the small-scale

faults identified in the toe region of Central slide fairway is parallel to the sliding direction and they are produced due to the shearing when the slide moving downslope (Fig. 6c), which also provides evidence for the slow-down of the slide.

In summary, the sediment transported by the Agadir Slide was: a) almost entirely trapped in the slide fairway and Agadir Canyon, and b) was not accelerated enough on the continental slope to disintergrate to form a turbidity current. The turbidites of the Moroccan Turbidite System must have another source. No other major landslide scars have been identified in the Agadir Canyon Region. This leaves the head region of the Agadir Canyon as the most likely source for the turbidites in the Moroccan Turbidite System despite the fact that only small failure scars (<5 km^3) can be identified in the head region of the canyon.

9. Discussion

9.1 Emplacement processes of the Agadir Slide

The morphological features and internal architecture of the Agadir Slide, when combined with our age constraints, provide important evidences to the emplacement of the Agadir Slide. The Agadir Slide did not affect the present-day seafloor and it is draped by recent sediments (Figs. 5b and 9a). The dating of the gravity cores in the study area provides an age of ~142±1 ka for the main slide body (Fig. 9b). The bathymetric data and seismic profiles of the Agadir Slide illustrate the presence of two headwall areas (the upper and lower headwall areas) at different water depths and two basal shear surfaces (BSS I and BSS II) at different stratigraphic depths. One key question is whether the Agadir Slide resulted from a single-phase event or from multi-stage failures. In order to gain a better understanding on the emplacement processes of the Agadir Slide, the following key observations should be taken into consideration:

(a) The Central slide fairway is cutting to the Western slide fairway and the BSS II is deeper than BBS I (Figs. 5a and b). The

western boundary (sidewall scarp) of the Central slide fairway is quite steep (up to 18°) (Fig. 3b).

(b) The seismic records display that the lower headwall area was not buried by the later deposits from the upper headwall area (Fig. 5a).

Here, three possible scenarios or hypotheses are proposed to investigate the emplacement processes of the Agadir Slide in the following sections.

The age model established in this study reveals that the Agadir Slide has an age of ~142±1 ka. The first scenario we may consider is that the Agadir Slide may be formed by a single-phase event but occurred along two basal shear surfaces (glide planes). Several previous studies have revealed that multiple mass wasting events can be triggered at the same time and amalgamate or erode each other (Moscardelli et al., 2006; Li et al., 2017). If this was the case for the Agadir Slide, the upper and lower headwall areas would have been generated simultaneously. The mobilised slide deposits along the BSS I in the Western slide fairway would have affected or covered the western boundary (sidewall scarp) of the Central slide fairway. However, as mentioned in the observation (a), the western sidewall scarp in the Central slide fairway is quite steep and no clear evidence can be shown on the seismic record that the sidewall scarp was covered or buried by slide deposits from the Western slide fairway (Fig. 5b). This may lead to the conclusion that the Agadir Slide may not be generated by one single-phase event, which produced two headwall areas almost at the same time.

Submarine landslides developed retrogressively in multiple episodes of slope failures have been documented by several case studies, e.g. the Hinlopen Slide (Vanneste et al., 2006), the Mauritania Slide Complex (Antobreh and Krastel, 2007), the Storegga Slide (Haflidason et al., 2004) and the Sahara Slide (Li et al., 2017). If the Agadir Slide was assumed to have been occurred in two slide phases retrogressively, the first slide event would have been triggered in the lower headwall area along the BSS II, and the slide deposits transported downslope in the Central

slide fairway and then entered in the Agadir Canyon. The second slide event would have been triggered in the upper headwall area retrogressively along the BSS I and the lower headwall area would be at least partly buried by the slide deposits from the upper headwall area. However, this is inconsistent with the observation (b) mentioned above. Thus, the Agadir Slide is not considered to have occurred in two phases retrogressively.

The third hypotheses for the emplacement processes of the Agadir Slide still considers that the Agadir Slide would have occurred in two slide events at ~142±1 ka, although exact time interval (< 2 ka) between these two phases is difficult to determine. The first slide event was triggered in the upper headwall area and pronounced sidewall scarps were generated as a result (Fig. 10a). Approximately 36 km^3 of seafloor sediment was mobilised, leading to an almost complete evacuation of sediment in the headwall area. The mobilised sediment was transported downslope and deposition was confined by several seamounts (e.g. SM1 to SM4). Most of the slide deposits travelled between SM 2 and SM 4, and only a minor amount of slide deposits were transported to the west of SM 2 and to the east of SM 4 (Fig. 10a). The slide deposits continued beyond SM 2 and SM 4 and were divided into two parts downslope (Fig. 10a). The slide deposits in the western part were transported into the Western slide fairway and later spread out, leading to the generation of positive topography at its western border (Fig. 10a). The eastern part of the slide deposits were further confined when passing between SM3 and SM4 (Fig. 10a).

The second phase of the Agadir Slide was initiated in the southern part of the Central slide fairway, i.e. between SM3 and SM4 (Fig. 10b and c). Here, a pronounced headwall scarp with a height of ~100 m was identified in the lower headwall area (Fig. 4b). The latter slide event produced the distinguished sidewall scarps of the Central slide fairway by reworking the eastern part of western slide fairway (Fig. 6b). The slide deposits were further transported downslope and entered into the pre-existing fairway in the northern

part (Fig. 7a). This led to the formation of pronounced sidewall scarps, which are most likely produced by enhanced erosion before the slide entered the Agadir Canyon (Fig. 10b). The increase of slope gradient from 0.5° to 1.8° at the transition from the fairway to the Agadir canyon likely promoted the further transportation of the slide deposits into the Agadir Canyon (Fig. 6b).

9.2 Could the Agadir Slide be the source of turbidite events in the Moroccan Turbidite System?

Submarine landslides and debris flows may transform to turbidity currents on both active and passive continental margins (Wynn et al., 2002; Trofimovs et al., 2008; Clare et al., 2014). Some large-volume submarine landslides (involving >100 km^3 of sediment) can rapidly disintegrate into far-travelling turbidity currents across very gentle slopes (Talling et al., 2007b). Flow transformation from debris flows to turbidity currents was reported, for instance, during the 1929 Grand Banks submarine landslide (Piper et al., 1999). The Moroccan Turbidite System offshore NW African margin has hosted numerous landslide-triggered turbidity currents over the past 200 ka (Wynn et al., 2002; Talling et al., 2007a; Hunt et al., 2013a). Most of these turbidity currents were sourced from the Moroccan margin, and were transported into the Moroccan Turbidite System via the Agadir Canyon (e.g. AB5, AB7 and AB12).

The Agadir Slide is the first identified large-scale submarine landslide in close vicinity to the Agadir Canyon (Krastel et al., 2016). So could the Agadir Slide be the source area of one of the turbidite events in the Moroccan Turbidite System? Several lines of evidences have been proposed to assess the relationship between the Agadir Slide and the turbidite events recorded in the Moroccan Turbidite System. For the past 200 ka, fourteen (14) turbidite events (AB1 to AB14) have been reported in the Moroccan Turbidite System (Wynn et al. 2002; Talling et al. 2007a; Hunt et al. 2013a). Turbidite AB12 was dated at 120 ka (early OIS5) and turbidite AB13 was deposited in the late OIS6,

approximately 135 ka ago (Wynn et al. 2002; Hunt et al. 2013a). Turbidite AB14 is a volcaniclastic turbidite deposited at ~165 ka, and is associated with the Icod landslide (Frenz et al. 2009; Hunt et al. 2013a). Our magnetic susceptibility stratigraphy provides an age of ~142±1 ka for the Agadir Slide, which is older than the closest turbidite AB13 by 7 ky. Even assuming a conservative error of 5 kyr (c.f. Urlaub et al., 2013) for AB13, making it ~140 ka, the Agadir Slide is recorded significantly below the 140 ka horizon (Fig. 9b). Therefore, it is certainly older than 140 ka and it does not correlate to any turbidites found down slope in the Moroccan Turbidite System. This means the Agadir Slide was not a source for turbidites in the Moroccan Turbidite System.

Most of turbidites coming from the Moroccan margin and filling the intraslope basin occurred mainly during the sea-level fall and lowstand stages (Urlaub et al., 2013). The Agadir Slide took place at ~142±1 ka during the sea-level lowstand stage. Urlaub et al. (2013) have proposed that there was no close relationship between the occurrence of submarine landslides and sea-level variations based on a data set of ages for 68 large volume submarine landslides. Therefore, it is difficult to determine if sea level variation was one of the controlling factors for the occurrence of Agadir Slide. Considering the identification of two basal shear surfaces (glide planes) for Agadir Slide, we propose that the preconditioning factor for Agadir Slide could be the presence of these two weak layers. Seismicity related to the fault activity and halokinesis can be considered as the plausible triggers for the occurrence of Agadir Slide. Similar cases have been documented in the Gulf of Mexico, where the occurrence of salt deformation and submarine landslides are also pervasive (Beaubouef and Abreu, 2010). Earthquakes related to salt deformation may play a critical role in initiating slope failures (Justin and Brandon, 2010).

10. Conclusions

High-resolution multibeam bathymetry

data, 2D seismic profiles and gravity cores allowed us to investigate the morphology, internal character, and origin of the Agadir Slide on the NW African margin. The main conclusions of this study are:

(1) The Agadir Slide affected an area of 5500 km^2, displaced a volume of 340 km^3 and shows a (run-out) distance of 350 km. The Agadir Slide includes two headwall areas, Western slide fairway and Central slide fairway.

(2) Volume calculations reveal that most of the Agadir Slide deposits, approximately 170 km^3, were accumulated in the Central and Western slide fairways, while ~70 km^3 of slide deposits were trapped in the Agadir Canyon.

(3) The Agadir Slide was emplaced at ~142 ka in two main phases. The first phase of Agadir Slide was triggered in the upper headwall area and the second phase occurred in the lower headwall area. The presence of two weak layers likely preconditioned the Agadir Slide, and seismicity associated with fault activity and halokinesis are considered to be the main triggers of the Agadir Slide.

(4) Salt structures affecting the seafloor have played a vital role on the distribution and evolution of the Agadir Slide. The slide does not correlate with turbidites down slope in the Moroccan Turbidite System. Therefore, the slide is interpreted to have travelled relatively slowly, and not disintegrated into a fluid turbidity current. The source of turbidites into the Moroccan Turbidite System is therefore likely to be in the head of the Agadir Canyon.

The detailed investigation of the Agadir Slide on the NW African margin reveals that not all submarine landslides can transform into turbidity currents. This will be an important case-study for the better understanding of the flow behavior of submarine landslides on other continental margins. It is also essential to access the hazards and risks of submarine landslides by integrating multi-disciplinary approaches.

References

Alves, T.M., 2015. Submarine slide blocks and associated soft-sediment deformation in deep-water basins: A review. Marine and Petroleum Geology 67, 262-285.

Alves, T.M., Strasser, M., Moore, G.F., 2014. Erosional features as indicators of thrust fault activity (Nankai Trough, Japan). Marine Geology 356, 5-18.

Antobreh, A.A., Krastel, S., 2007. Mauritania Slide Complex: morphology, seismic characterisation and processes of formation. International Journal of Earth Sciences 96, 451-472.

Beaubouef, R.T., Abreu, V., 2010. MTCs of the Brazos-Trinity Slope System; Thoughts on the Sequence Stratigraphy of MTCs and Their Possible Roles in Shaping Hydrocarbon Traps, in: Mosher, D.C., Shipp, R.C., Moscardelli, L., Chaytor, J.D., Baxter, C.D.P., Lee, H.J., Urgeles, R. (Eds.), Submarine Mass Movements and Their Consequences. Springer Netherlands, Dordrecht, pp. 475-490.

Clare, M.A., Talling, P.J., Challenor, P., Malgesini, G., Hunt, J., 2014. Distal turbidites reveal a common distribution for large (>0.1 km3) submarine landslide recurrence. Geology 42, 263-266.

Dugan, B., 2012. Petrophysical and consolidation behavior of mass transport deposits from the northern Gulf of Mexico, IODP Expedition 308. Marine Geology 315-318, 98-107.

Dunlap, D.B., Wood, L.J., Weisenberger, C., Jabour, H., 2010. Seismic geomorphology of offshore Morocco's east margin, Safi Haute Mer area. AAPG Bulletin 94, 615-642.

Frenz, M., Wynn, R.B., Georgiopoulou, A., Bender, V.B., Hough, G., Masson, D.G., Talling, P.J., Cronin, B.T., 2009. Provenance and pathways of late Quaternary turbidites in the deep-water Agadir Basin, northwest African margin. International Journal of Earth Sciences 98, 721-733.

Freudenthal, T., Meggers, H., Henderiks, J., Kuhlmann, H., Moreno, A., Wefer, G., 2002. Upwelling intensity and filament activity off Morocco during the last 250,000 years. Deep Sea Research Part II: Topical Studies in Oceanography 49, 3655-3674.

Frey Martinez, J., Cartwright, J., Hall, B., 2005. 3D seismic interpretation of slump complexes: examples from the continental margin of Israel. Basin Research 17, 83-108.

Gamboa, D., Alves, T., Cartwright, J., Terrinha, P., 2010. MTD distribution on a 'passive' continental margin: The Espírito Santo Basin (SE Brazil) during the Palaeogene. Marine and Petroleum Geology 27, 1311-1324.

Gee, Masson, Watts, Allen, 1999. The Saharan debris flow: an insight into the mechanics of long runout submarine debris flows. Sedimentology 46, 317-335.

Georgiopoulou, A., Masson, D.G., Wynn, R.B., Krastel, S., 2010. Sahara Slide: Age, initiation, and processes of a giant submarine slide. Geochemistry, Geophysics, Geosystems 11, 1-22.

Haflidason, H., Sejrup, H.P., Nygård, A., Mienert, J., Bryn, P., Lien, R., Forsberg, C.F., Berg, K., Masson, D., 2004. The Storegga Slide: architecture, geometry and slide development. Marine Geology 213, 201-234.

Hampton, M.A., Lee, H.J., Locat, J., 1996. Submarine landslides. Reviews of Geophysics 34, 33-59.

Harbitz, C.B., Parker, G., Elverhøi, A., Marr, J.G., Mohrig, D., Harff, P.A., 2003. Hydroplaning of subaqueous debris flows and glide blocks: Analytical solutions and discussion. Journal of Geophysical Research: Solid Earth 108 (B7).

Hühnerbach, V., Masson, D.G., 2004. Landslides in the North Atlantic and its adjacent seas: an analysis of their morphology, setting and behaviour. Marine Geology 213, 343-362.

Hunt, J.E., Wynn, R.B., Talling, P.J., Masson, D.G., 2013a. Frequency and timing of landslide-triggered turbidity currents within the Agadir Basin, offshore NW Africa: Are there associations with climate change, sea level change and slope sedimentation rates? Marine Geology 346, 274-291.

Hunt, J.E., Wynn, R.B., Talling, P.J., Masson, D.G., 2013b. Turbidite record of frequency and source of large volume (>100 km3) Canary Island landslides in the last 1.5 Ma: Implications for landslide triggers and geohazards. Geochemistry, Geophysics, Geosystems 14, 2100-2123.

Imbrie, J., Hays, J. D., Martinson, D. G., McIntyre, A., Mix, A. C., Morley, J.J. et al, 1984. The orbital theory of Pleistocene climate: support from a revised chronology of the marine δ18O record. In A. Berger, J. Imbrie, H. Hays, G. Kukla, B. Saltzman (Ed.): Milankovitch and Climate: Understanding the Response to

Astronomical Forcing. Proceedings of the NATO Advanced Research Workshop held 30 November - 4 December, 1982 in Palisades, NY. Dordrecht: D. Reidel Publishing.

Justin, S., Brandon, D., 2010. Overpressure and earthquake initiated slope failure in the Ursa region, northern Gulf of Mexico. Journal of Geophysical Research: Solid Earth 115.

Krastel, S., Behmann, J.-H., Völker, D., Stipp, M., Berndt, C., Urgeles, R., Chaytor, J., Huhn, K., Strasser, M., Harbitz, C.B., 2014. Submarine mass movements and their consequences. 6th International Symposium. Advances in Natural and Technological Research 37, pp 683.

Krastel, S., Wynn, R.B., Georgiopoulou, A., Geersen, J., Henrich, R., Meyer, M., Schwenk, T., 2012. Large-Scale Mass Wasting on the Northwest African Continental Margin: Some General Implications for Mass Wasting on Passive Continental Margins. 189-199.

Krastel, S., Wynn, R.B., Feldens, P., Schürer, A., Böttner, C., Stevenson, C., Cartigny, M.J.B., Hühnerbach, V., Unverricht, D., 2016. Flow Behaviour of a Giant Landslide and Debris Flow Entering Agadir Canyon, NW Africa, in: Lamarche, G., Mountjoy, J., Bull, S., Hubble, T., Krastel, S., Lane, E., Micallef, A., Moscardelli, L., Mueller, C., Pecher, I., Woelz, S. (Eds.), Submarine Mass Movements and their Consequences: 7th International Symposium. Springer International Publishing, Cham, pp. 145-154.

Kuhlmann, H., Freudenthal, T., Helmke, P., Meggers, H., 2004. Reconstruction of paleoceanography off NW Africa during the last 40,000 years: influence of local and regional factors on sediment accumulation. Marine Geology 207, 209-224.

Li, W., Alves, T.M., Urlaub, M., Georgiopoulou, A., Klaucke, I., Wynn, R.B., Gross, F., Meyer, M., Repschläger, J., Berndt, C., Krastel, S., 2017. Morphology, age and sediment dynamics of the upper headwall of the Sahara Slide Complex, Northwest Africa: Evidence for a large Late Holocene failure. Marine Geology 393, 109-123.

Masson, D.G., 1994. Late Quaternary turbidity current pathways to the Madeira Abyssal Plain and some constraints on turbidity current mechanisms. Basin Research 6, 17-33.

Masson, D.G., Harbitz, C.B., Wynn, R.B., Pedersen, G., Løvholt, F., 2006. Submarine landslides: processes, triggers and hazard prediction. Philosophical Transactions of the Royal Society A: Mathematical, Physical and Engineering Sciences 364, 2009-2039.

Moscardelli, L., Wood, L., 2008. New classification system for mass transport complexes in offshore Trinidad. Basin Research 20, 73-98.

Moscardelli, L., Wood, L., 2015. Morphometry of mass-transport deposits as a predictive tool. GSA Bulletin 128 (1-2): 47-80.

Moscardelli, L., Wood, L., Mann, P., 2006. Mass-transport complexes and associated processes in the offshore area of Trinidad and Venezuela. AAPG Bulletin 90, 1059-1088.

Mosher, D.C., Moscardelli, L., Shipp, R.C., Chaytor, J.D., Baxter, C.D.P., Lee, H.J., Urgeles, R., 2010. Submarine Mass Movements and Their Consequences, in: Mosher, D.C., Shipp, R.C., Moscardelli, L., Chaytor, J.D., Baxter, C.D.P., Lee, H.J., Urgeles, R. (Eds.), Submarine Mass Movements and Their Consequences. Springer Netherlands, Dordrecht, pp. 1-8.

Ochoa, J., Wolak, J., Gardner, M.H., 2013. Recognition criteria for distinguishing between hemipelagic and pelagic mudrocks in the characterization of deep-water reservoir heterogeneity. AAPG Bulletin 97, 1785-1803.

Owen, M., Day, S., Long, D., Maslin, M., 2010. Investigations on the Peach 4 Debrite, a Late Pleistocene Mass Movement on the Northwest British Continental Margin, in: Mosher, D.C., Shipp, R.C., Moscardelli, L., Chaytor, J.D., Baxter, C.D.P., Lee, H.J., Urgeles, R. (Eds.), Submarine Mass Movements and Their Consequences. Springer Netherlands, Dordrecht, pp. 301-311.

Piper, D.J.W., Cochonat, P., Morrison, M.L., 1999. The sequence of events around the epicentre of the 1929 Grand Banks earthquake: initiation of debris flows and turbidity current inferred from sidescan sonar. Sedimentology 46, 79-97.

Piper, D.J.W., Pirmez, C., Manley, P.L., Long, D., Food, R.D., Normark, W.R., Showers, W., 1997. Mass-transport deposits of the Amazon Fan. In: Flood, R.D., Piper, D.J.W., Klaus, A., Peterson, L.C. (Eds.), Proceedings of the Ocean Drilling Program, Scientific Results, Vol. 155, pp. 109-146.

Rothwell, R.G., Pearce, T.J., Weaver, P.P.E., 1992. Late Quaternary evolution of the Madeira Abyssal Plain, Canary Basin, NE Atlantic. Basin Research 4, 103-131.

Sawyer, D.E., Flemings, P.B., Dugan, B., Germaine, J.T., 2009. Retrogressive failures recorded in mass transport deposits in the Ursa Basin, Northern Gulf of Mexico. Journal of Geophysical Research 114.

Seibold, E., 1982, The northwest African continental margin-An introduction, in U. Von Rad, K. Hinz, M. Sarnthein, and E. Seibold, eds., Geology of the northwest African continental margin: Berlin, Springer-Verlag, p. 215–269.

Smith, W.H.F., Wessel, P., 1990. Gridding with continuous curvature splines in tension. Geophysics 55, 293-305.

Stevenson, C.J, Talling, P.J., Wynn, R.B., Masson, D.G., Hunt, J.E., Frenz, M., Akhmetzhanov, A., and Cronin, B.T., 2013, The flows that left no trace: Very large-volume turbidity currents that bypassed sediment through submarine channels without eroding the sea floor: Marine and Petroleum Geology 41, 186-205

Stevenson, C.J., Talling, P.J., Masson, D.G., Sumner, E.J., Frenz, M., and Wynn, R.B., 2014. The spatial and temporal distribution of grain-size breaks in turbidites. Sedimentology 61, 1120-1156.

Sun, Q., Alves, T., Xie, X., He, J., Li, W., Ni, X., 2017. Free gas accumulations in basal shear zones of mass-transport deposits (Pearl River Mouth Basin, South China Sea): An important geohazard on continental slope basins. Marine and Petroleum Geology 81, 17-32.

Talling, P.J., Amy, L.A., Wynn, R.B., 2007a. New insight into the evolution of large-volume turbidity currents: comparison of turbidite shape and previous modelling results. Sedimentology 54, 737-769.

Talling, P.J., Wynn, R.B., Masson, D.G., Frenz, M., Cronin, B.T., Schiebel, R., Akhmetzhanov, A.M., Dallmeier-Tiessen, S., Benetti, S., Weaver, P.P., Georgiopoulou, A., Zuhlsdorff, C., Amy, L.A., 2007b. Onset of submarine debris flow deposition far from original giant landslide. Nature 450, 541-544.

Tappin, D.R., Grilli, S.T., Harris, J.C., Geller, R.J., Masterlark, T., Kirby, J.T., Shi, F., Ma, G., Thingbaijam, K.K.S., Mai, P.M., 2014. Did a submarine landslide contribute to the 2011 Tohoku tsunami? Marine Geology 357, 344-361.

Tari, G., Jabour, H., 2013. Salt tectonics along the Atlantic margin of Morocco. Geological Society, London, Special Publications 369, 337-353.

Thomson, J., Weaver, P.P.E., 1994. An AMS radiocarbon method to determine the emplacement time of recent deep-sea turbidites. Sedimentary Geology 89, 1-7.

Trofimovs, J., Sparks, R.S.J., Talling, P.J., 2008. Anatomy of a submarine pyroclastic flow and associated turbidity current: July 2003 dome collapse, Soufrière Hills volcano, Montserrat, West Indies. Sedimentology 55, 617-634.

Urlaub, M., Talling, P.J., Masson, D.G., 2013. Timing and frequency of large submarine landslides: implications for understanding triggers and future geohazard. Quaternary Science Reviews 72, 63-82.

Vanneste, M., Mienert, J., Bunz, S., 2006. The Hinlopen Slide: A giant, submarine slope failure on the northern Svalbard margin, Arctic Ocean. Earth and Planetary Science Letters 245, 373-388.

Watt, S.F.L., Talling, P.J., Vardy, M.E., Heller, V., Hühnerbach, V., Urlaub, M., Sarkar, S., Masson, D.G., Henstock, T.J., Minshull, T.A., Paulatto, M., Le Friant, A., Lebas, E., Berndt, C., Crutchley, G.J., Karstens, J., Stinton, A.J., Maeno, F., 2012. Combinations of volcanic-flank and seafloor-sediment failure offshore Montserrat, and their implications for tsunami generation. Earth and Planetary Science Letters 319-320, 228-240.

Wefer, G. and cruise participants, 1997. Report and preliminary results of METEOR-Cruise M37/1, Lisbon-Las Palmas, 4.12.-23.12.1996. Berichte aus dem Fachbereich Geowissenschaften der Universität Bremen, 090. Department of Geosciences, Bremen University.

Wien, K., Kölling, M., Schulz, H.D., 2007. Age models for the Cape Blanc Debris Flow and the Mauritania Slide Complex in the Atlantic Ocean off NW Africa. Quaternary Science Reviews 26, 2558-2573.

Wynn, R.B., Masson, D.G., Stow, D.A.V., Weaver, P.P.E., 2000. The Northwest African slope apron: a modern analogue for deep-water systems with complex seafloor topography. Marine and Petroleum Geology 17, 253-265.

Wynn R.B., Talling P.J., Masson D.G., Stevenson C.J., Cronin B.T., Bas T.P.L. (2010) Investigating the Timing, Processes and Deposits of One of the World's Largest Submarine Gravity Flows: The 'Bed 5 Event' Off Northwest Africa. In: Mosher D.C. et al. (eds) Submarine Mass Movements and Their Consequences. Advances in Natural and Technological Hazards Research, vol 28. Springer, Dordrecht.

Wynn, R.B., Weaver, P.P.E., Masson, D.G., Stow, D.A.V., 2002. Turbidite depositional architecture across three interconnected deep-water basins on the north-west African margin. Sedimentology 49, 669-695.
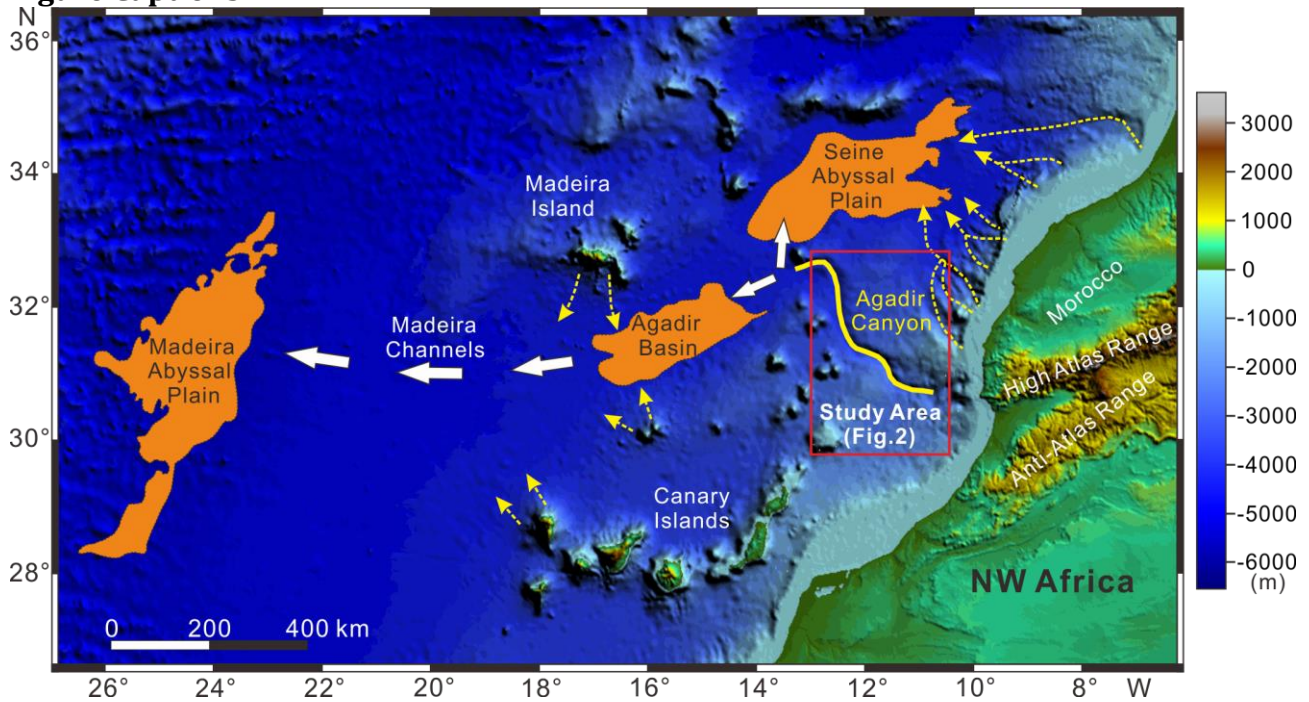
Fig. 1 Combined bathymetric and topographic map showing key geomorphological features offshore the Northwest African continental margin (e.g. Canary Islands, Madeira Island, High Atlas Range and Anti-Atlas Range). The red box highlights the location of the study area. The yellow solid line indicates the course of the Agadir Canyon (Wynn et al., 2000). The Moroccan Turbidite System extends through three interconnected basins, marked in orange in the figure: the Seine Abyssal Plain, the Agadir Basin, and the Madeira Abyssal Plain. The yellow dashed lines indicate the principal transport directions for turbidity currents entering the Morocco Turbidite System (modified after Wynn et al., 2002).
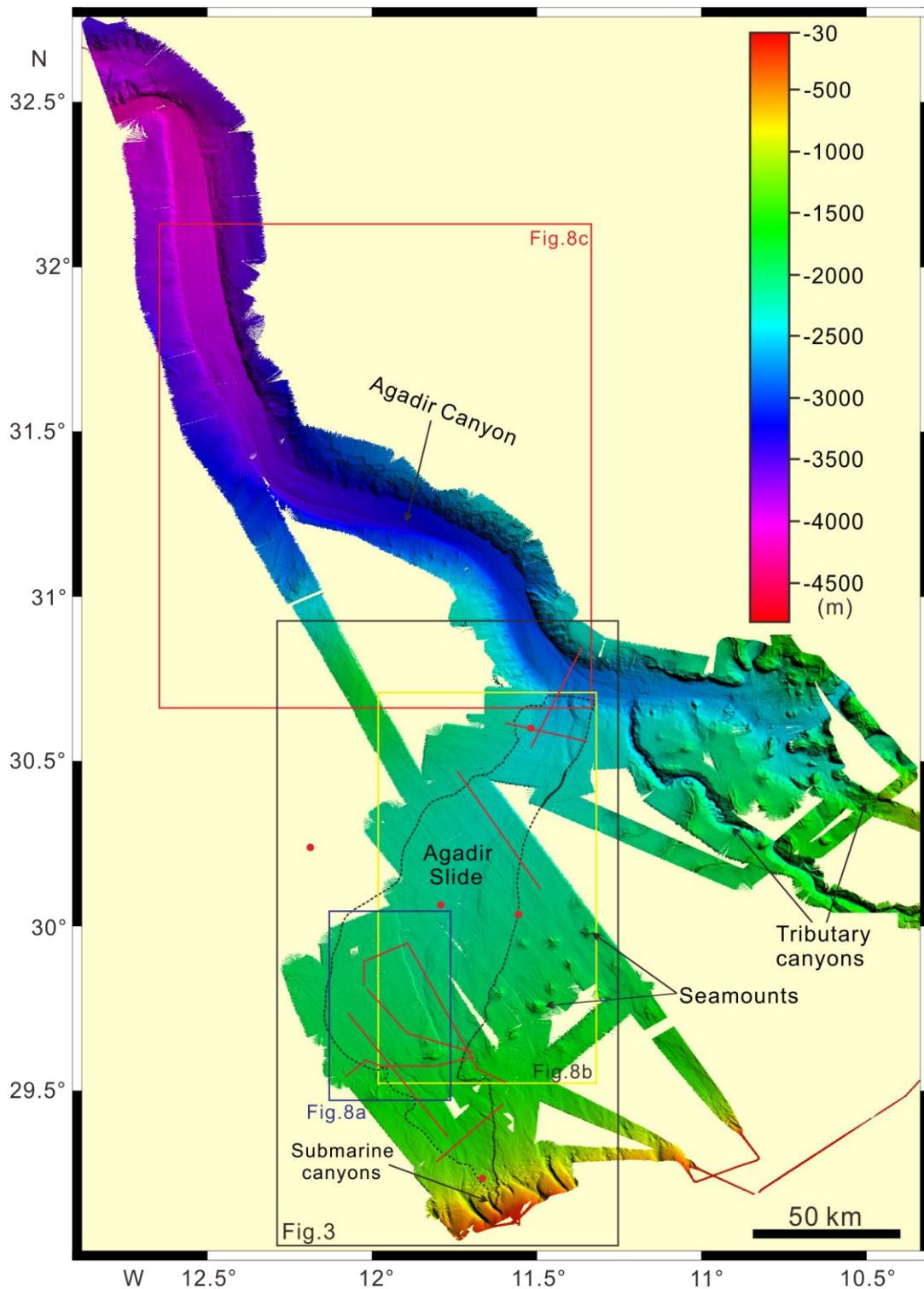
Fig. 2 Multibeam bathymetric map of the study area illustrating the distribution and seafloor morphology of the Agadir Canyon and the Agadir Slide. Several tributary canyons are identified at the headwall of the Agadir Canyon. The boxes with different colours represent the locations of figures used in the following sections of this work. The black dashed line indicates the boundary of the Agadir Slide.
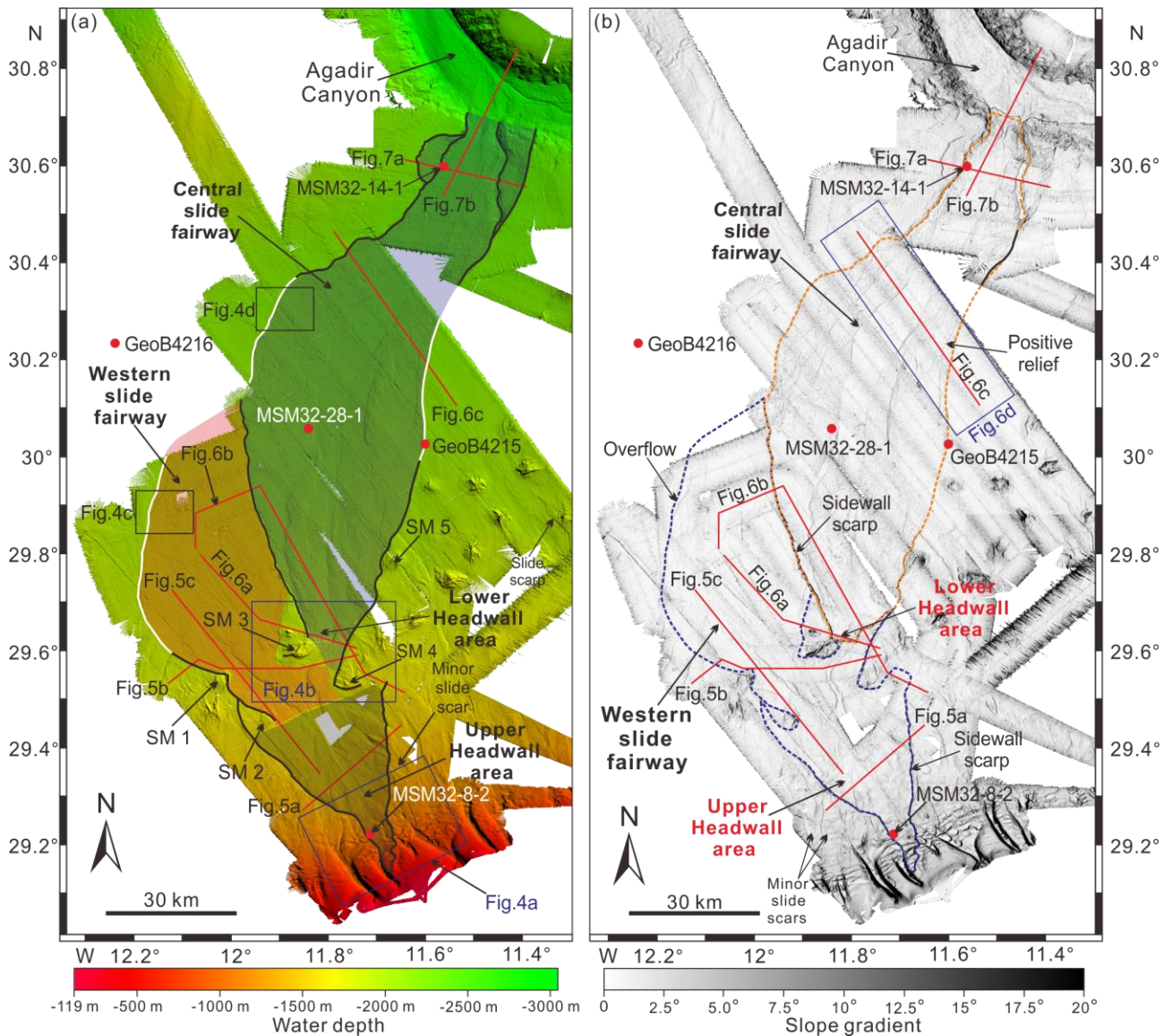
Fig. 3 (a) High-resolution multibeam bathymetric map showing the detailed seafloor morphology of the Agadir Slide. The red solid lines indicate the locations of 2D seismic data shown in this paper. Five major seamounts are also marked in the figure. The black solid lines indicate the escarpment of Agadir Slide. The white solid lines represent the locations of positive reliefs. (b) Slope gradient map of the Agadir Slide area revealing two pronounced headwall areas and associated sidewall scarps. The red circles represent the location of the gravity cores described in this paper. The purple and orange dashed lines indicate the distribution of BSS I and BSS II, respectively.
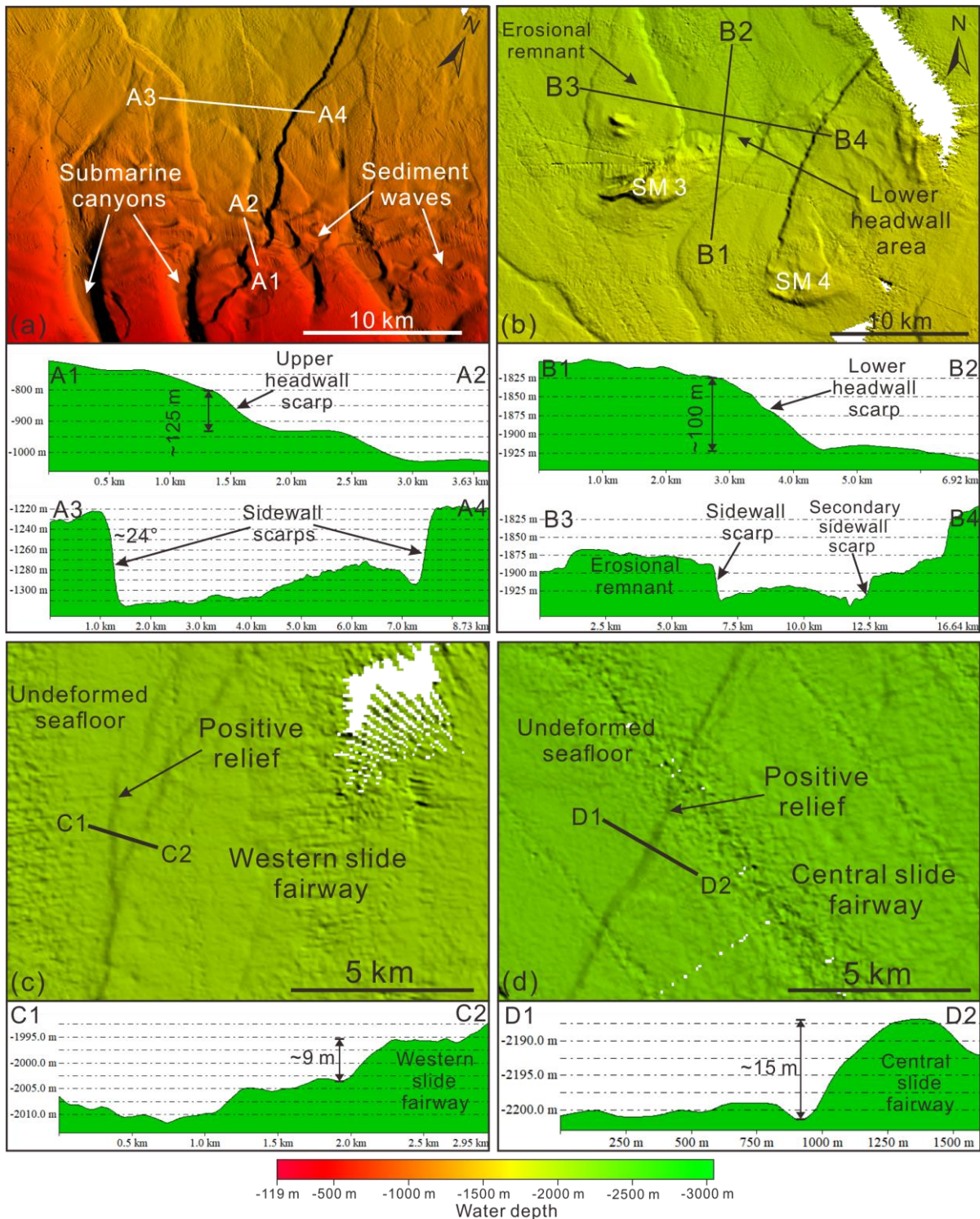
Fig. 4 (a) Multibeam bathymetric map showing the detailed seafloor morphology of the upper headwall area. Submarine canyons and a field of sediment waves can be observed in the upslope area. The headwall scarp and sidewall scarps in the upper headwall area can be illustrated on the topographical profiles A1-A2 and A3-A4, respectively. (b) Detailed geomorphology of the lower headwall area showing the seamounts (SM 3 and 4) and an erosional remnant in the downslope region of SM 3. Topographical profiles B1-B2 and B3-B4 revealing the headwall scarp sidewall scarps in the lower headwall area. (c) Positive relief can be imaged in the Western slide fairway on the bathymetrical map and shows a height difference of ~9 m on the topographical profile C1-C2. (d) Multibeam bathymetric map showing the positive relief in the Central slide fairway with a height difference of ~15 m on the topographical profile D1-D2. Please see the locations of bathymetric maps in Fig. 3a.
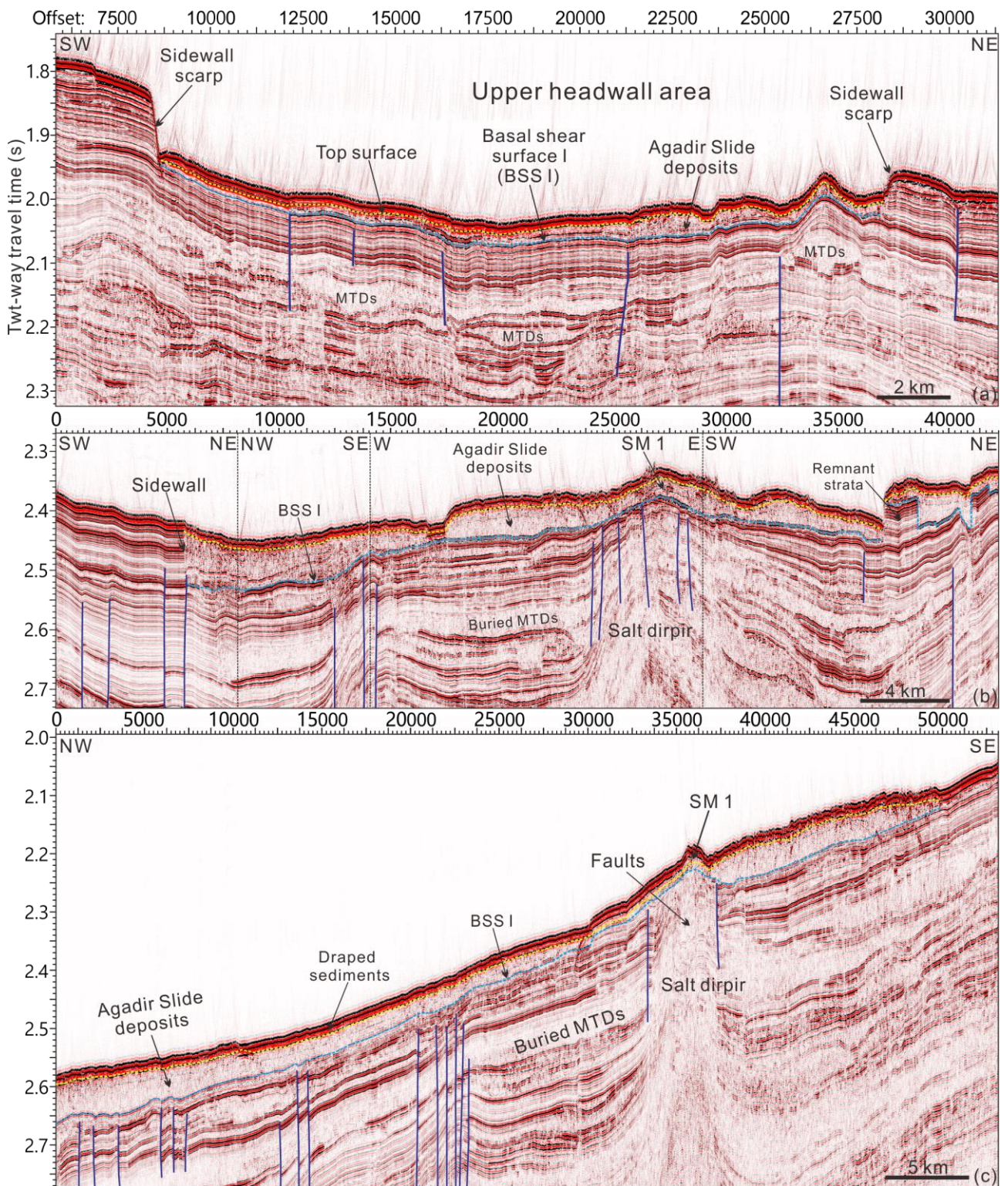
Fig. 5 (a) Two-dimensional (2D) seismic profile across the headwall area of Agadir Slide showing sidewall scarps and multiple mass-transport deposits (MTDs). The blue and yellow, dashed lines indicate the base and top surface of the Agadir Slide, respectively. Note that the slide deposits in the headwall area are very thin, as this region was almost entirely evacuated. (b) Two-dimensional (2D) seismic profile crossing the Western slide and Central slide fairways from west to east. The profile highlights the relatively thick Agadir Slide deposits and a developed salt diapir underneath the Agadir Slide. (c) Two-dimensional (2D) seismic profile, oriented SE-NW, and crossing the upper headwall area and the Western slide fairway. The figure reveals how markedly the Agadir slide deposits are separated by salt diapir in parts of the headwall area.
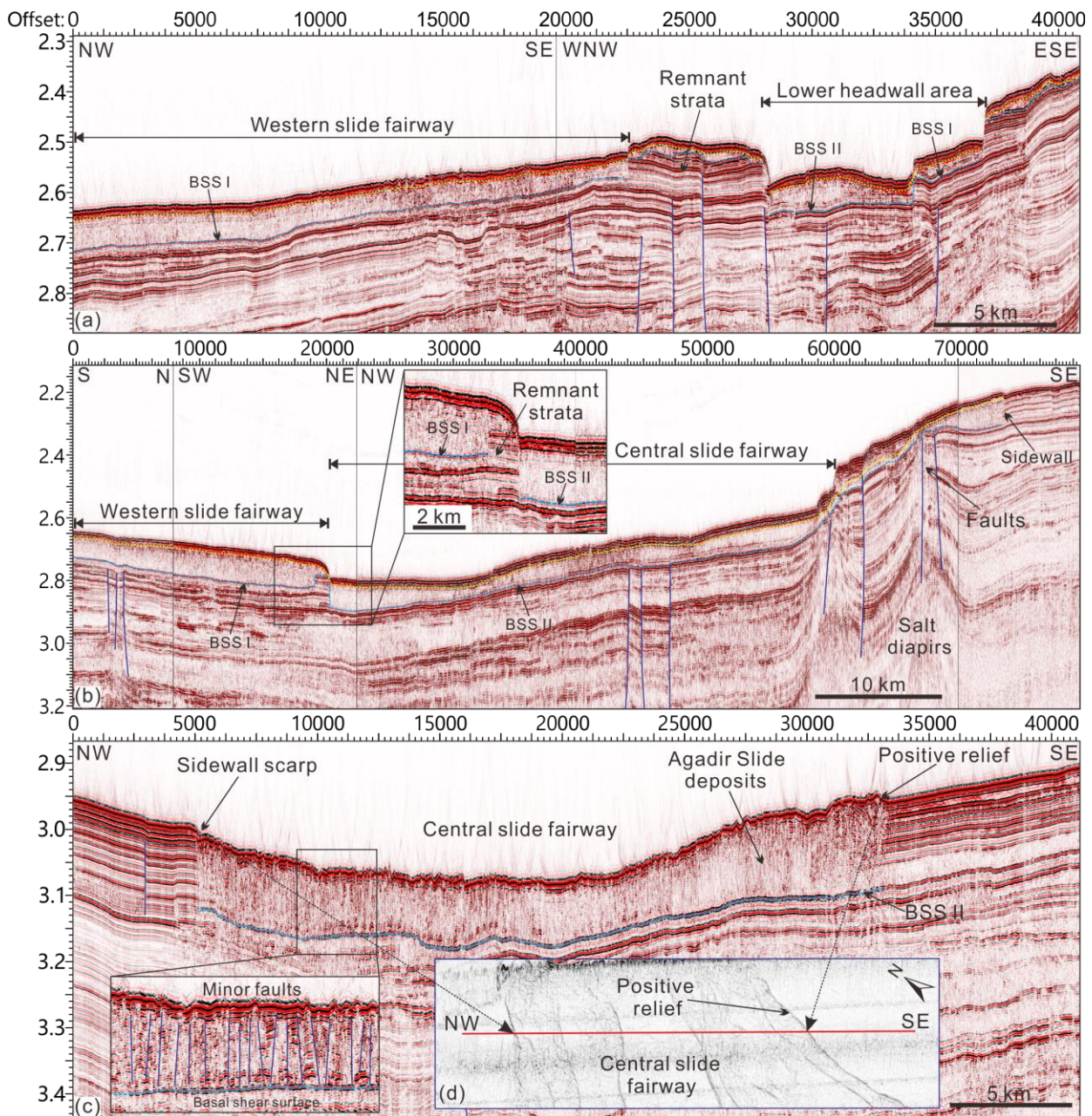
Fig. 6 (a) Two-dimensional (2D) seismic profile crossing the Western slide fairway and the Central slide fairway, from northwest to southeast. This seismic profile shows the basal shear surfaces (BSS I and II) of Agadir Slide rooted at different stratigraphic depths. Note that numerous faults are identified below the Agadir Slide deposits. (b) Two-dimensional (2D) seismic profile denoting thicker slide deposits in the Western slide fairway compared to those in the Central slide fairway. Note once again the distinct stratigraphic depths of the basal shear surfaces in both areas and the undisturbed strata in-between. (c) Two-dimensional (2D) seismic profile across the Central slide fairway revealing a sidewall scarp to the northwest, and slide deposits with a positive morphology to the southeast. Several buried MTDs are observed underneath the Agadir Slide deposits. (d) Slope gradient map showing the positive relief in the toe region of the Central slide fairway (Please see location in Fig. 3b).
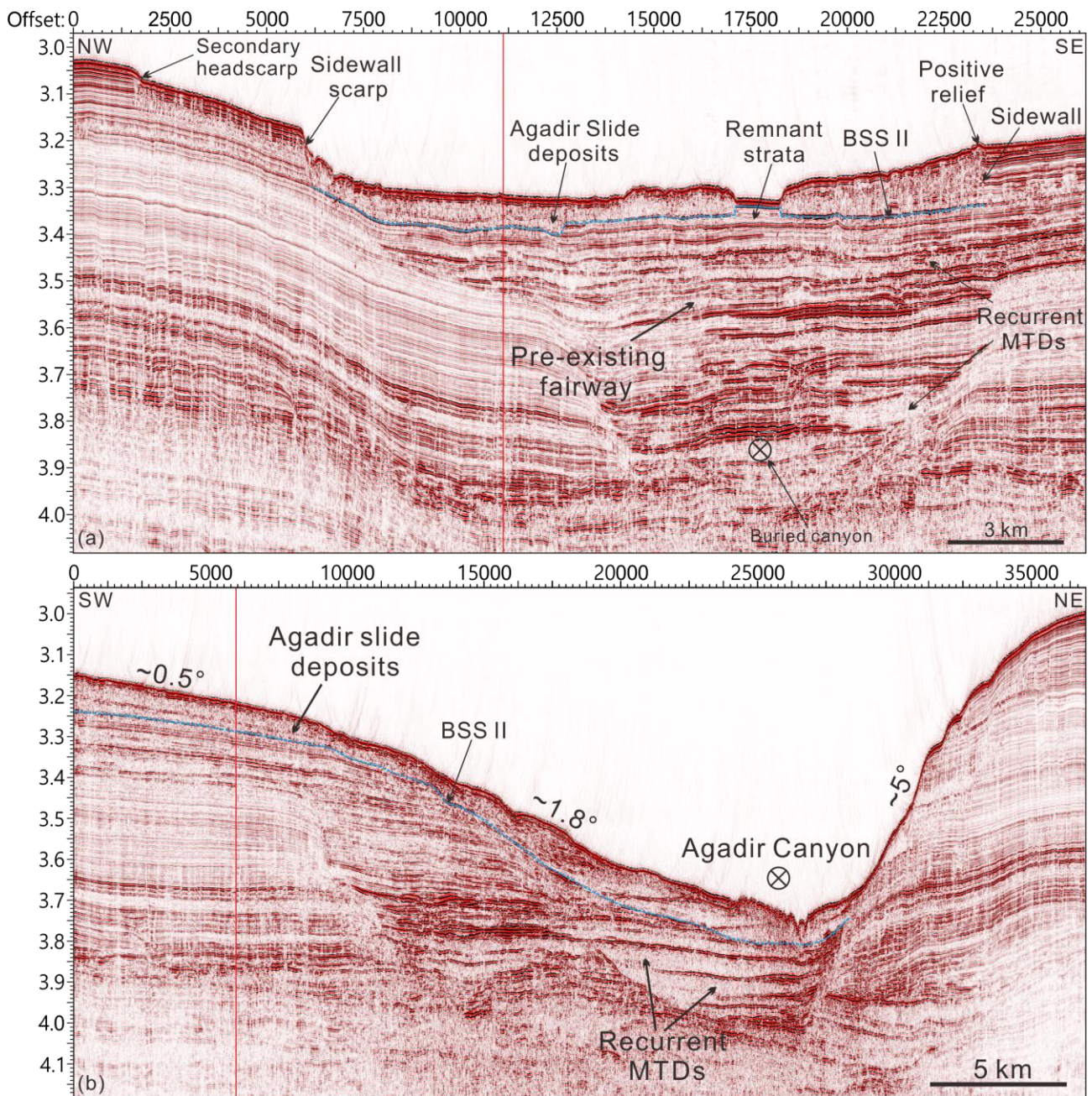
Fig. 7 (a) Two-dimensional (2D) seismic profile crossing the southern part of the Central slide fairway. The profile reveals a buried submarine canyon filled by multiple MTDs, and a secondary headwall scarp to the northwest. Note that slide deposits show positive relief compared to the adjacent undisturbed strata. (b) Two-dimensional (2D) seismic profile across the southernmost part of the Central slide fairway. In this location, the Agadir Canyon shows multiple stacked MTDs in its interior. The NE flank of the Agadir Canyon is much steeper than its SW counterpart.
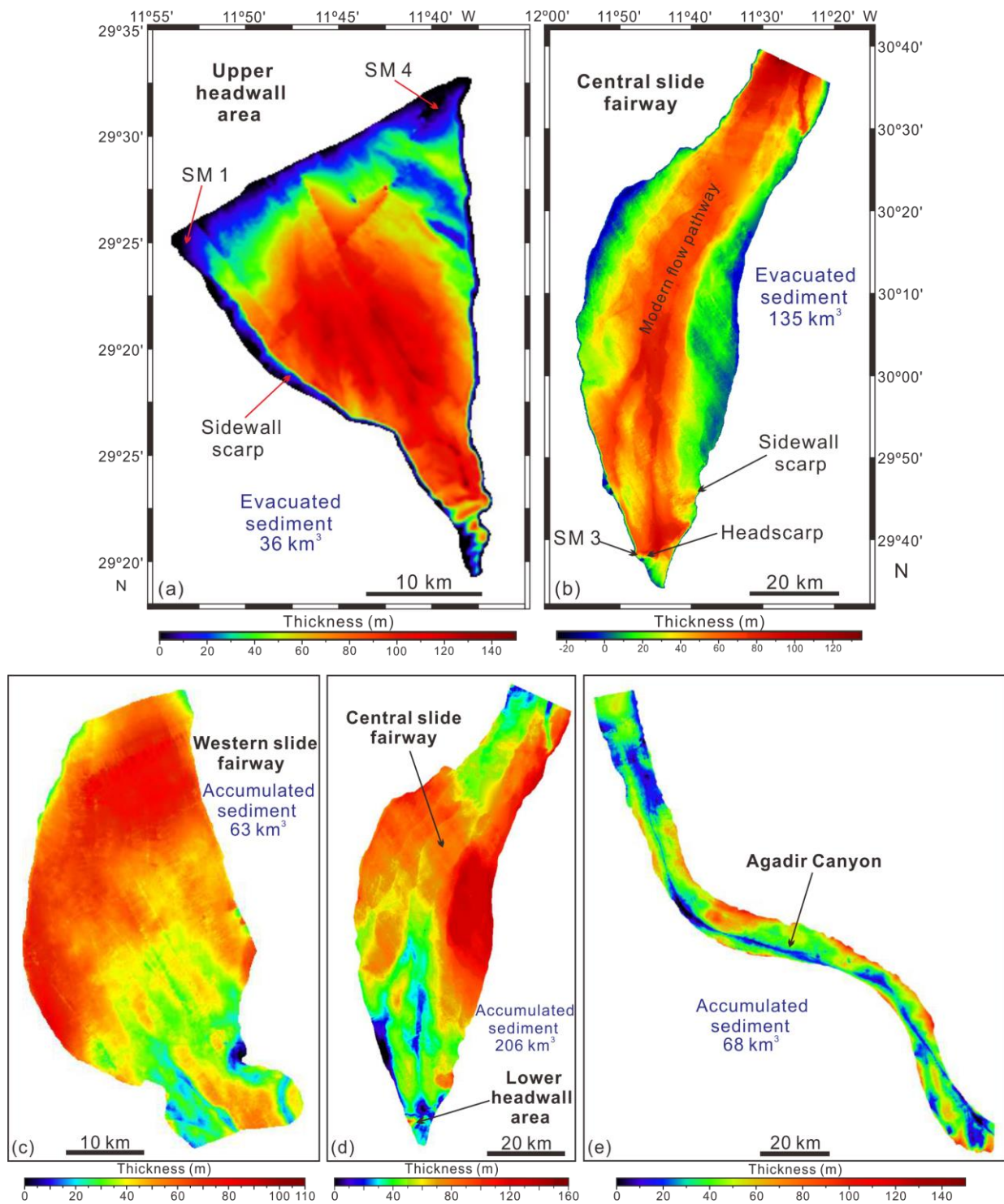
Fig. 8 (a) Thickness map of the evacuated sediments in the headwall area revealing that a volume of 36 km³ and a thickness of up to 140 m of sediment were removed from the headwall area. (b) Thickness map of evacuated (mobilized) sediments in the Central slide fairway revealing that most of the sediments were displaced along its axis. The negative values at the flanks of the Central slide fairway indicate slide deposits accumulated higher than the surrounding unaffected sea floor. (c) Thickness map of the slide deposits in the Western slide fairway showing that the majority of slide deposits are located in its northern part. (d) Thickness map of the slide deposits in the Central slide fairway revealing a complex sediment distribution. Note that most of the slide deposits in this region are identified close to the eastern and western borders of the Central slide fairway. (e) Thickness map of the slide deposits trapped within the Agadir Canyon.
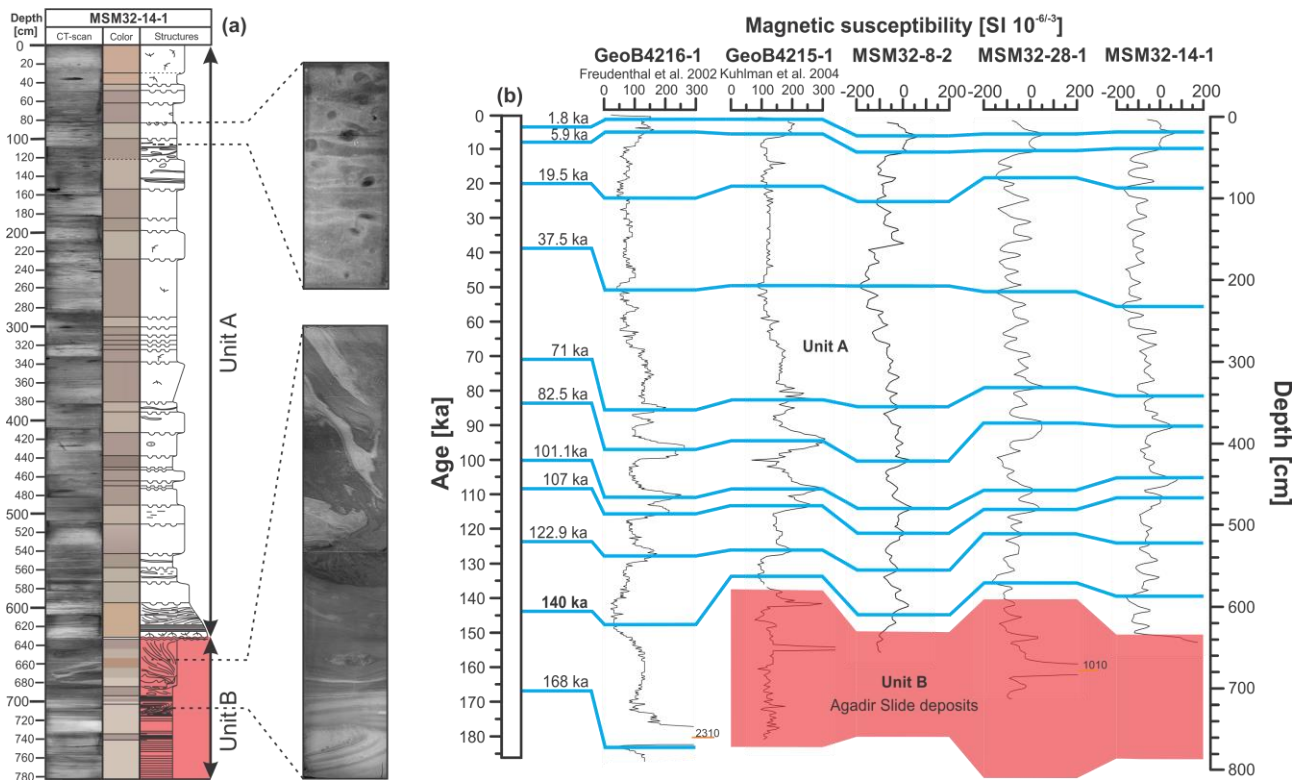
Fig. 9 (a) CT-scan and visual description of gravity core MSM32-14-1 illustrate the colour and sedimentary structures. Unit A represents a continuous succession of hemipelagic sediment and Unit B (marked in red) indicates the Agadir Slide deposits. The zoomed section reveals the remobilized sediment. (b) Sediment-core correlations across the study area of the Agadir Slide. Unit B represents the Agadir Slide deposits (marked in red). Blue lines correlate Magnetic Susceptibility tie-points along the full transect. The respective ages of each tie-point in cores GeoB 4216-1 and GeoB 4215-2 were extracted from the data sets in Freudenthal et al. (2002) and Kuhlman et al. (2004).
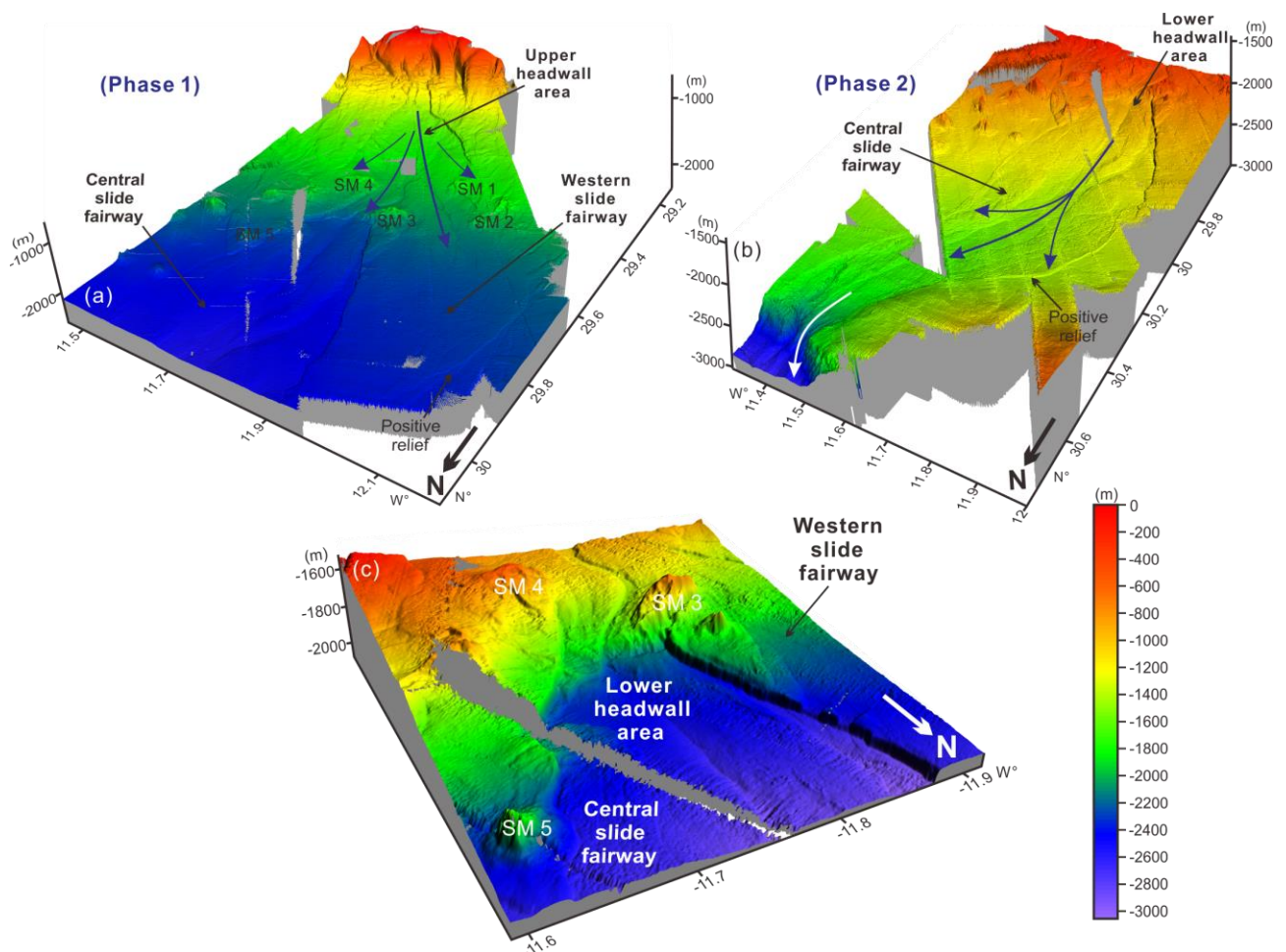
Fig. 10 Three-dimensional morphological model illustrating the key emplacement processes in the Agadir Slide. (a) The first phase of Agadir Slide was triggered in the upper headwall area and the slide deposits were diverted by the seamounts. The blue arrows indicate the mass movement directions. (b) The second phase of Agadir Slide was triggered in the lower headwall area and slide deposits were transported downslope entering the Agadir Canyon. (c) 3D bathymetric view of the lower headwall area.